Drug Development and Industrial Pharmacy, 2011; 37(11): 1339–1346

ISSN 0363-9045 print/ISSN 1520-5762 online
DOI: 10.3109/03639045.2011.575162

informa
healthcare

RESEARCH ARTICLE

Enhanced cellular uptake of folic acid–conjugated PLGA–PEG nanoparticles loaded with vincristine sulfate in human breast cancer

Jianian Chen, Shaoshun Li, Qi Shen, Huijuan He, and Yi Zhang

School of Pharmacy, Shanghai Jiao Tong University, Shanghai, China

Abstract

The aim of this paper is to evaluate the cellular uptake of vincristine sulfate-loaded poly(lactic-co-glycolic acid)–polyethylene glycol (PLGA–PEG) nanoparticles with the folic acid modification (PLGA–PEG–folate NPs). PLGA–PEG–folate NPs were prepared using a water–oil–water emulsion solvent evaporation method. The particle size, surface morphology, drug encapsulation efficiency, and the drug release behavior were investigated. The NPs exhibited a biphasic drug release with a moderate initial burst followed by a sustained release profile. Internalization of the NPs labeled with coumarin-6 by MCF-7 (Michigan Cancer Foundation-7) human breast cancer cells was quantitatively measured by microplate reader, and qualitatively analyzed by fluorescent microscopy and confocal laser scanning microscopy. The results showed PLGA–PEG–folate NPs achieved significantly higher cellular uptake in the folic acid receptor overexpressed MCF-7 cells, compared to PLGA–mPEG NPs without the folic acid modification. Due to the enhanced cellular uptake, PLGA–PEG–folate NPs displayed the highest cytotoxicity. Judged by IC_{50} after 24 h culture, the therapeutic effects of the drug formulated in the NPs with surface modification could be 1.52 times, 3.91 times higher than that of PLGA–mPEG NPs and free vincristine sulfate, respectively.

Keywords: Cellular uptake, folic acid, conjugation, PLGA–PEG, nanoparticle, vincristine sulfate

Introduction

In the last decade, ligand-modified nanoparticle drug delivery systems loaded with anticancer agents have received considerable attention for their site-specific targeting capacity[1–3]. A variety of ligands have been used to immobilize on the surface of nanosized polymeric carriers to deliver these nanoparticles (NPs) into cells mainly *via* receptor-mediated endocytosis. Among these targeting moieties used in drug delivery systems, folic acid is widely employed[4–7]. Folic acid as a targeting ligand offers many potential advantages: small size; convenient availability and low cost; relatively simple and defined conjugation chemistry; high receptor affinity, and a lack in normal tissue receptor expression, which gives it high tumor tissue specificity[8].

Vincristine sulfate (VCR), extracted from the plant *Vinca rosea*, is an effective chemotherapeutic agent that has been used extensively for the treatment of a number of human carcinomas including acute leukemia, malignant lymphoma, and breast cancer. Dose-dependent and cumulative peripheral neuropathy, however, is the main dose-limiting side effect of chemotherapy[9,10]. Tumor-targeted drug delivery systems are considered options that can overcome the nonspecific targeting characteristics and reduce the side effects of VCR. It was reported that the therapeutic activity of VCR could be significantly enhanced after its encapsulation in a liposome[11]. PLGA and poly(lactic acid), which have been approved by the US Federal Drug Administration, are extensively used as pharmaceutical materials because of their biocompatibility and biodegradability[12]. PEG-modified PLGA (PLGA–PEG) NPs have been developed over the years because they show tremendous potential as long circulating systems[13,14].

Though the folic acid–conjugated liposome[15–17], NPs[18,19], micelles[20,21] are extensively applied to enhance the anti-tumor effect of the drug, few concerns the cellular uptake of folate-modified PLGA–PEG NPs loaded with

Address of Correspondence: Dr. Qi Shen, School of Pharmacy, Shanghai Jiao Tong University, Dongchuan Road 800, Shanghai, 200240, China. E-mail: qshen@sjtu.edu.cn

(Received 13 October 2010; revised 08 January 2011; accepted 20 March 2011)

VCR[22]. The aim of this study is to investigate the cellular uptake of PLGA–PEG–folate NPs using several *in vitro* techniques. In detail, based on the polymeric carriers PLGA–mPEG and PLGA–PEG–folate, PLGA–PEG–folate NPs were prepared *via* a slightly modified water–oil–water emulsion solvent evaporation method. The *in vitro* release behavior of VCR was studied. The cellular uptake of PLGA–PEG–folate NPs in MCF-7 (Michigan Cancer Foundation-7) human breast cancer cells was quantitatively and qualitatively analyzed. Finally, the *in vitro* cytotoxicity of PLGA–PEG–folate NPs against MCF-7 cells was investigated. By comparing PLGA–PEG–folate NPs with other formulations of VCR (PLGA–mPEG NPs and free VCR), we hope to determine whether PLGA–PEG NPs with the folic acid modification are able to enhance the cellular uptake of VCR *in vitro* or not.

Methods and materials

Materials

For the synthesis of polymer NPs, poly(ethylene glycol) (HO-PEG-OH, MW 2000 Da) and methoxy poly(ethylene glycol) (mPEG-OH, MW 2000 Da) were purchased from Sigma-Aldrich (USA). Tris base was obtained from Amresco (USA). VCR was obtained from Shanghai Anticancer Phytochemistry Co., Ltd. (China). Poly(D, L-lactide-co-glycolide) (50 mol% of lactide, MW 15 kDa) (PLGA–COOH), D, L-lactic acid, and glycolic acid were purchased from Daigang Corporation (Shandong Province, China). Coumarin 6, folic acid, polyvinyl alcohol 1788 (PVA 1788, average MW 88,000, CPS: 4.6–5.4), and other reagents were purchased from Aladdin Reagent (China) Co., Ltd.

Molecular weights of the synthesized PLGA–mPEG samples were measured on a Perkin-Elmer 200 series (USA) of gel permeation chromatography. Fourier transform infrared spectroscopy data were acquired at room temperature using an EQUNOX 55 system with a DTGS detector (Bruker, Germany) over the range of 4000–370 cm^{-1}. Scanning electron microscope (SEM) images were obtained using a field emission scanning electron microscope (FEI SIRION 200/INCA OXFORD, USA FEI/UK OXFORD). Three kinds of instruments including Varioskan Flash microplate reader (Thermo, USA), Olympus IX-71 inverted microscope (Olympus Corp., Japan), and TCS SP5 laser scanning confocal microscope (Leica, Germany) were introduced to study the cellular uptake of the NPs.

For cell culture experiments, MCF-7 human breast cancer cells were purchased from the Institute of Biochemistry and Cell Biology, Shanghai Institutes for Biological Sciences (China). 3-(4,5-dimethylthiaol-2-yl)-2,5-diphenyltetrazolium bromide (MTT) was obtained from Sigma-Aldrich.

Synthesis of the polymers PLGA–mPEG and PLGA–PEG–folate

The PLGA–mPEG copolymers were synthesized by ring-opening polymerization[23,24] and PLGA–PEG–folate was synthesized *via* the conjugation of PLGA–PEG–NH_2 with the activated folic acid which was described previously[25–27].

Preparation and characterization of VCR-loaded NPs

VCR-loaded NPs

Because VCR is amphiphilic, we prepared PLGA–PEG–folate NPs by water–oil–water emulsion solvent evaporation method with slight modifications[28–30]. Briefly, 1.0 mL of Tris–HCl buffer (pH 6–7.4) containing 10 mg VCR was emulsified in 15 mL of ethyl acetate/chloroform (v:v = 1:1) containing 190 mg polymeric carriers (PLGA–mPEG and PLGA–PEG–folate, w/w = 4:1) by sonication over an ice-bath using a Scientz-II D ultrasonic probe (Ningbo Scientz Biotechnology Corp., China) at an output of 90 W for 30 s. The primary emulsion was added to 200 mL of 1.0% (w/v) PVA 1788 solution (pH 6–7.4) and sonicated for 2 min to form a double emulsion. Organic solvent residues were removed by stirring at room temperature and evaporating under reduced pressure. The nanodroplets were centrifuged at 15,000 rpm for 1 h to remove free VCR (F-VCR) in the system. To investigate the cellular uptake of VCR-loaded NPs, the fluorescent coumarin- 6 loaded NPs were prepared *via* the addition of coumarin 6 during the formation of the primary emulsion. PLGA–mPEG NPs were prepared by a similar procedure: PLGA–mPEG was used instead of the above two polymeric carriers; and drug-free NPs (blank PLGA–PEG–folate NPs and blank PLGA–mPEG NPs) were prepared *via* the same procedure.

Characterization of particle size and ζ potential

To determine particle size and ζ potential, the nanoparticle suspension was diluted and measured using a 90Plus particle size analyzer (Brookhaven Instruments Corporation, USA). The nanoparticle suspension was analyzed by autocorrelation to determine both mean size and ζ potential. All measurements were performed in triplicate.

Morphology study

The morphological examination of NPs was performed using a scanning electron microscope. A drop of the dilute nanoparticle suspension was placed onto a copper sheet and then dried under reduced pressure at 40°C. For SEM analysis, the surfaces of the corresponding membranes were sputtered with gold in a vacuum before viewing under the microscope.

Evaluation of drug content

The obtained nanoparticle suspension was frozen and lyophilized in a freeze-drier system to obtain the NPs. The drug loading and entrapment efficiency of VCR in NPs was determined as follows: 500 mg of the lyophilized NPs was evenly dispersed in 100 mL of physiological saline, and NPs concentration was obtained (5 mg/mL). Ten microlitre of the sample was sucked out from the nanoparticle suspension, then 90 μL of dimethyl

sulfoxide (DMSO) was added to destruct the NPs. After the sample was vortexed for 30 s, 900 μL methanol was add to precipitate insoluble polymers. After the mixture was vortexed again and centrifuged, the supernatant was filtered using a 0.45 μm Millipore filter and subjected to hihg-performance liquid chromatography (HPLC) analysis to determine the drug concentration. The result is defined as drug concentration encapsulated into the NPs. The mobile phase of the HPLC consisted of a mixture of 0.02 M aqueous dipotassium hydrogen phosphate–methanol (14:86, v/v) at a flow rate of 0.7 mL/min; pH was adjusted to 6.7. The column effluent was detected at 267 nm with a UV–Vis detector (LC-20AT Shimadzu, Japan). Finally, using the following formulas (1) and (2), the drug loading and entrapment efficiency of VCR in NPs could be determined. The measurements were performed in triplicate.

$$\text{Drug loading (\%)} = (\text{drug concentration encapsulated into the NPs}/5) \times 100 \quad (1)$$

$$\text{Entrapment efficiency (\%)} = \frac{(\text{drug concentration encapsulated into the NPs})}{(\text{total drug concentration})} \times 100 \quad (2)$$

In the formula, the number 5 represents the concentration of the final nanoparticle suspension. Total drug concentration can be calculated using the following equation: total drug concentration = (total drug amount added during the procedure)/(the dispersion volume); the dispersion volume refers to the physiological saline volume (100 mL) where lyophilized NPs are dispersed.

In vitro drug release behavior

To evaluate the *in vitro* release behavior of VCR from folate-modified PLGA–PEG NPs, Tris–HCl buffer solution was selected, and a dialysis technique was used. In brief, 1 mL of VCR-loaded PLGA–PEG nanoparticle suspension [the drug loading was calculated according to the above formula (1)] was placed in a dialysis bag (MWCO 1000) and dialyzed against 30 mL of the release medium with 100 ± 2 rpm at 37 ± 0.5°C. At predetermined time intervals (including time zero), 300 μL of the solution outside the dialysis bag was removed for analysis and replaced with a fresh buffer solution. The removed samples were immediately frozen and stored at –70°C until analysis. The samples were detected by HPLC. The percentage of drug released from NPs was plotted against time and the cumulative amount of VCR was calculated. All measurements were performed in triplicate.

Cell culture and cellular uptake

Cellular uptake study by microplate reader

To quantitatively evaluate the uptake of the NPs, MCF-7 human breast cancer cells were used. MCF-7 cells were seeded in 96-well black plates. After the cells reached 70–80% confluency, the medium in the wells was replaced with 100 μL of freshly coumarin 6-loaded nanoparticle suspension (the loading rate was 0.15%). The concentrations of the nanoparticle suspension in the wells were 100, 200, 300, 400, and 500 μg/mL, respectively; and the cells were incubated for 1 h. After the suspension was removed, the cells were washed with phosphate-buffered saline (PBS) three times to eliminate traces of NPs left in the wells. Then, 0.5% Triton X-100 in 0.1 N NaOH was introduced into each well to lyse the cells. The fluorescence intensity of each sample well was measured by microplate reader with excitation wave length at 450 nm and emission wavelength at 490 nm[31]. The amount of NPs (μg) in the cell lysates was calculated according to the concentration of coumarin 6. The total cell protein content in each well was determined using BCA protein assay; a standard curve was obtained with bovine serum albumin solution. The cellular uptake efficiency of NPs by MCF-7 cells was expressed as the amount of NPs (μg) uptaken per mg cell protein[32]. In a separate experiment, to study the effect of receptor competition on the uptake, the cells were preincubated with 30 μg/mL of folic acid for 1 h at 37°C, and then incubated with the coumarin 6-loaded NPs suspension for 0.5, 1, 1.5, 2, and 4 h, respectively. The following procedures were the same as described above. All measurements were performed in triplicate.

Fluorescence microscope and confocal laser scanning microscopy

For qualitative study, after MCF-7 cells were co-incubated with coumarin 6 samples in 24-well plates, the cells were rinsed with cold PBS for three times, and then fixed by ethanol for 20 min. The cells were further washed twice with PBS and the nuclei were counterstained with propidium iodide (PI) for 15 min. Then, the cells were washed twice with PBS and observed under a fluorescence microscope. To study the localization of NPs, MCF-7 cells were seeded on a glass slide at a density of 5×10^4 cells/mL and allowed to attach overnight. After the incubation with coumarin 6 samples, the cells were treated *via* the same procedures, and then placed on a mounting glass to be observed by TCS SP5 confocal laser scanning microscope.

In vitro cell cytotoxicity by MTT assay

MTT method was used to evaluate the cytotoxicity of VCR-loaded PLGA–PEG–folate NPs. In a 96-well plate, MCF-7 cells were seeded at a density of 5×10^4 cells/mL, then cultivated at 37°C for 8 h. Dulbecco's modified Eagle's medium was replaced by 100 μL fresh medium containing F-VCR, PLGA–mPEG NPs, and PLGA–PEG–folate NPs, respectively. After co-incubation for 24 h, 20 μL MTT solution in phosphate buffer solution (5 mg/mL) was added to each well, and the cells were incubated for another 4 h at 37°C in the dark. After drawing-off of the culture medium, 100 μL DMSO was added to dissolve formazan crystal; the percentage of cell viability was determined by measuring the absorbance (Abs) at $\lambda = 570$ nm using a microplate reader. Inhibitory rate was

calculated using the following equation, and IC_{50} values were obtained using Origin v8.0 (OriginLab Corp.).

$$\text{Inhibitory rate} = \frac{(\text{Abs}_{570}\text{control cells} - \text{Abs}_{570}\text{treated cells})}{\text{Abs}_{570}\text{control cells}} \times 100\%$$

All assays were conducted with four parallel samples. The IC_{50} values are defined as the drug concentrations that kill 50% of cells relative to controls.

Statistical analyses

Except where mentioned, data were presented as mean ± standard deviation (S.D.). One-way analysis of variance test was performed on the data to assess the impact of the formulation variables on the results ($n = 3$ or more). A p value of ≤0.05 was considered to be statistically significant.

Results and discussion

Characterization of the polymers PLGA–mPEG and PLGA–PEG–folate

The IR spectroscopy of the polymers PLGA–mPEG and PLGA–PEG–folate is shown in Figure 1. According to the previous reports[23,24], PLGA–mPEG was synthesized and characterized; the MW and the polydispersity (M_w/M_n) of the produced polymer were 15,342 and 1.41, respectively. To the polymer PLGA–PEG–folate, a prominent peak at 1759 cm^{-1} is corresponding to –C=O stretching in the polymers. Considering the spectra of folic acid–conjugated PLGA–PEG-NH_2, the presence of a slightly salient peak at 1623 cm^{-1} could be attributed to the formation of amide bond between amino group and carboxyl group. The conjugation percentage of folic acid in the polymer PLGA–PEG–folate was 20.1% based on a previously reported method[25].

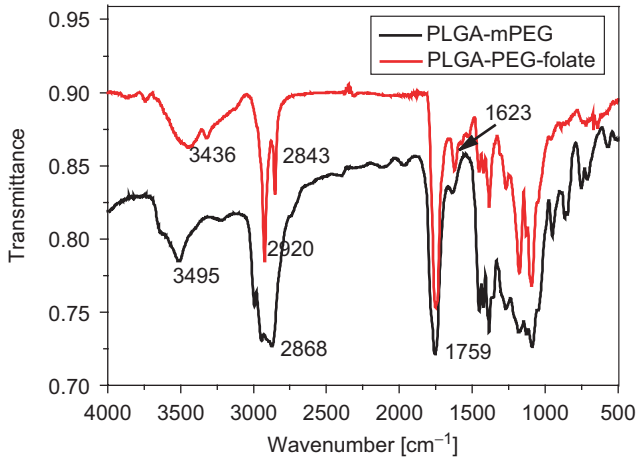

Figure 1. Infra-red spectra of polymer PLGA-mPEG and PLGA-PEG-folate. The presence of all major vibrational features associated with PLGA, PEG, and folate can be seen in the spectra. PEG, polyethylene glycol; PLGA, poly(lactic-co-glycolic acid).

Preparation and characterization of NPs loaded with VCR

We successfully prepared PLGA–PEG–folate NPs and PLGA–mPEG NPs using the water–oil–water emulsion solvent evaporation method[28-30]. The physical characteristics of VCR-loaded PLGA–PEG–folate NPs including the effective diameter, drug entrapment efficiency are shown in Table 1. The sizes of NPs were determined by a dynamic laser scattering method. The particle size of PLGA–PEG–folate NPs was measured to be 237.0 ± 16.1 nm. NPs demonstrated favorable stability as evidenced by ζ potentials below –10 mV. The SEM images of PLGA–PEG–folate NPs loaded with VCR in Figure 2 indicate that the particles exhibit to be a typical spherical with average size ~230 nm.

In vitro release

The *in vitro* release profiles of the NPs were investigated in Tris–HCl buffers (pH 6.8) at 37 ± 0.5°C. We found that folate-modified PLGA–PEG NPs exhibit typical biphasic release patterns: an initial burst release followed by a steady, continued-release pattern (Figure 3). Release was fast in the first 12 h, that is, 63.12 ± 3.51% VCR release from the NPs. In the following interval (12–60 h), a sustained release rate was observed. Within 24 h, the accumulative release was 70.19 ± 4.99% for folate-modified PLGA–PEG NPs. The initial burst may be associated with the rapid release of drugs deposited on the surface and in the water channels in NPs, whereas the steady release may be attributed to the diffusion of the drug localized in the PLGA core of the NPs.

In vitro cellular uptake

In this study, coumarin 6 was chosen as a fluorescence probe in fluorescence and confocal microscopic studies due to its low dye-loading requirement for NPs[33]. It is noted that, the entrapment efficiency of coumarin 6-loaded into PLGA–PEG NPs (including PLGA–mPEG NPs and PLGA–PEG–folate NPs) is very high maybe due to its very low hydrophilicity. In the experiment, it was found that the entrapment efficiency was over 98% in PLGA–PEG NPs. Moreover, the release of coumarin 6 from PLGA–PEG NPs was very slow, and within 24 h, the cumulative release was less than 5%. These results agree with the previous report[34]. We loaded coumarin 6 into the NPs to compare the cellular uptake of PLGA–PEG–folate NPs and PLGA–mPEG NPs by MCF-7 cells. The time- and

Table 1. Characterization of VCR-loaded PLGA–PEG–folate NPs.

Nanoparticles	Content of PVA (%, w/v)	Particle size (nm)	ζ potential (mV)	Drug loading (%)	Entrapment efficiency (%)
PLGA–PEG–folate NPs	1.0	237.0 ± 16.1	–13.27 ± 3.01	1.8 ± 0.2	46.7 ± 6.2

Results are expressed as the mean ± S.D. ($n = 3$).

concentration-dependent internalization of NPs by MCF-7 cells was observed (Figure 4). In the experiment, we found that within the low concentration range (100–350 μg/mL, here refers to the concentration of the NPs), the uptake of coumarin 6–loaded PLGA–PEG–folate NPs was much higher than that of coumarin 6–loaded PLGA–mPEG NPs. Compared to coumarin 6 NPs, coumarin 6 solution displayed the lowest uptake in the cells if coumarin 6 concentrations added to the wells were the same (cellular uptake data for coumarin 6 solution were not shown). But with the increase of the concentrations (>350 μg/mL of NPs), the difference of the fluorescence density in MCF-7 cells among the three kinds of the coumarin 6 formulations was becoming smaller and smaller. The uptake difference at low concentrations may be a direct result of surface modification: PLGA–PEG–folate NPs with the folic acid modification possess high affinity to the folic acid receptor, which allows the NPs to be easily taken up by the tumor cells where the folic acid receptor is highly expressed, therefore enhanced cellular uptake by MCF-7 cells is detected[35,36]. More importantly, PLGA–PEG–folate NPs enter the cells *via* folic acid receptor-mediated endocytosis mechanism which is significantly different from coumarin 6 solution[37,38]. This leads to longer retention time of coumarin 6–loaded PLGA–PEG–folate NPs within the cells as evidenced by increased fluorescence intensity. However, at higher concentrations, the intracellular uptake of coumarin 6 reached a peak value and its concentration no longer increased. This indicates that there is a saturated uptake phenomenon of the PLGA–PEG NPs. To verify the endocytosis mechanism of PLGA–PEG–folate

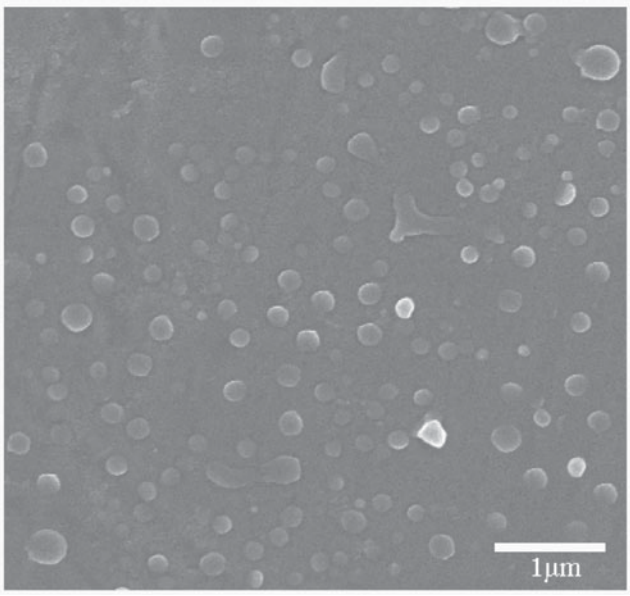

Figure 2. Scanning electron micrographs of PLGA–PEG–folate NPs loaded with VCR. Before viewing under the microscope, the surfaces of corresponding membranes were sputtered with gold. Images showed the nanoparticles with average size ~230 nm. NP, nanoparticle; PEG, polyethylene glycol; PLGA, poly(lactic-co-glycolic acid); VCR, vincristine sulfate.

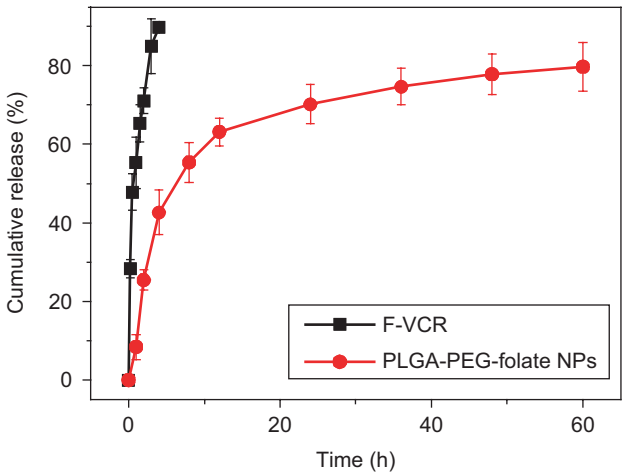

Figure 3. *In vitro* drug release profiles of VCR from folate-modified PLGA–PEG NPs in Tris-HCl buffer solution at pH 6.8 (37°C). NP, nanoparticle; PEG, polyethylene glycol; PLGA, poly(lactic-co-glycolic acid); VCR, vincristine sulfate.

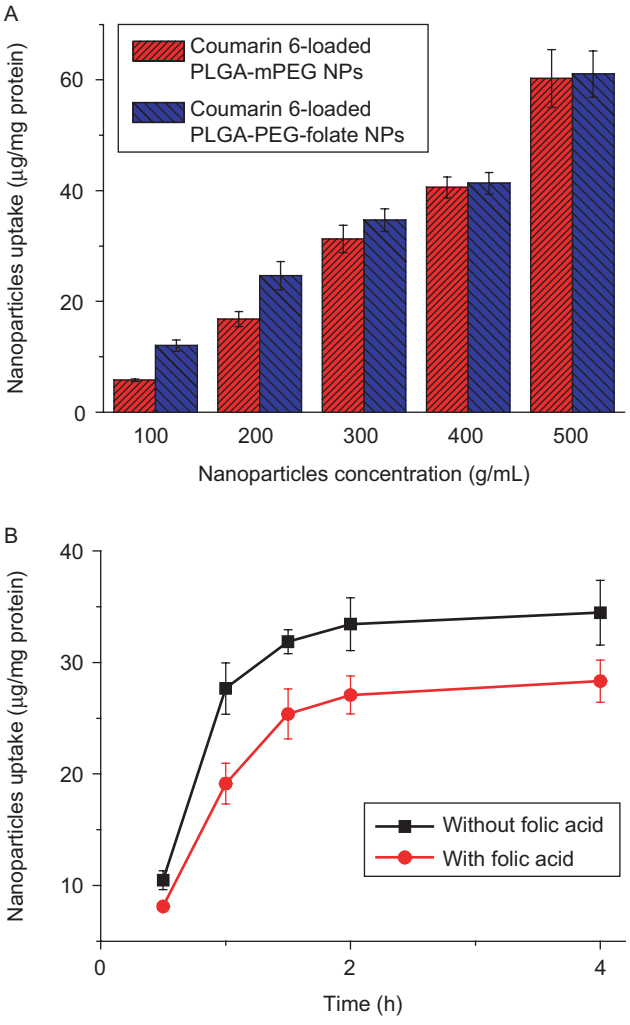

Figure 4. (A) Cellular uptake of coumarin 6–loaded PLGA–PEG NPs after 1 h by MCF-7 cells. (B) Cellular uptake of the coumarin 6–loaded PLGA–PEG–folate NPs with or without the pre-incubation of free folic acid. Values represent mean ± S.D. ($n = 3$). NP, nanoparticle; PEG, polyethylene glycol; PLGA, poly(lactic-co-glycolic acid); VCR, vincristine sulfate.

NPs mediated by folic acid receptor[38], excess free folic acid (30 μg/mL) was added to the wells and preincubated with MCF-7 cells for different time. The result is shown in Figure 4B. We could come to a conclusion that, compared to that of untreated group, the cellular uptake of PLGA–PEG–folate NPs evidently declined possibly because the endocytosis of the NPs were partially suppressed.

To qualitatively study the cellular uptake of the NPs, coumarin 6–labeled MCF-7 cells were visualized using fluorescence and confocal microscopy. The fluorescence images of internalized coumarin 6 are shown in Figure 5A. When the cells were incubated with coumarin 6 solution (400 ng/mL), a slight fluorescence signal was observed in the cells. Similarly, negligible fluorescence was observed when the cells were incubated with the blank NPs (dada not shown). But to the coumarin 6–loaded NPs (the concentration of coumarin 6 loaded into the NPs in each well was also 400 ng/mL, and the concentration of the NPs was about 267 μg/mL), the strong fluorescence signal was captured, and PLGA–PEG–folate NPs demonstrated the strongest green fluorescence. To study the intracellular localization of VCR-loaded NPs, we simultaneously loaded coumarin 6 and VCR into PLGA–PEG–folate NPs. As shown in Figure 5B, after MCF-7 cells were co-incubated with the NPs for 1 h and then counterstained with PI for 15 min, an obvious green fluorescence in the cell cytoplasm and red fluorescence around the nucleus were observed. Moreover, it was found that the red fluorescence in MCF-7 cells treated with the NPs for 4 h was much stronger than that for 1 h (Figure 5C). That is, the red fluorescence intensity increased with the increase of the incubation time in the first 4 h, which reflected the continuous penetration of NPs into the cells and a portion of them into the nuclei. So we speculate that PLGA–PEG–folate nanoparticulate carrier probably carry VCR-like active molecules across the cell membrane by endocytosis and transport effectively into the cells.

In vitro evaluation of cytotoxicity

Figure 6A shows the *in vitro* cytotoxicity of MCF-7 cells after the incubation with the VCR formulations: VCR aqueous solution, PLGA–mPEG NPs and PLGA–PEG–folate NPs at the concentration of 0.2, 0.5, 1, 5, 10, 30 nM, respectively ($n = 4$). The viability was measured by MTT assay. After a 24-h exposure of the cells to the drug, a dose-dependent reduction in growth rate was observed. At the same concentration, VCR-loaded NPs showed higher cytotoxicity than did F-VCR. A significant difference ($p < 0.05$) in the viability of the cells within the range of 1–30 nM was observed. PLGA–PEG–folate NPs displayed the highest cytotoxicity; the order of the cytotoxicity was PLGA–PEG–folate NPs > PLGA–mPEG NPs > F-VCR. The IC_{50} values decreased from 10.24 ± 1.52 nM for F-VCR to 3.99 ± 0.23 nM for PLGA–mPEG NPs, then to 2.62 ± 0.19 nM

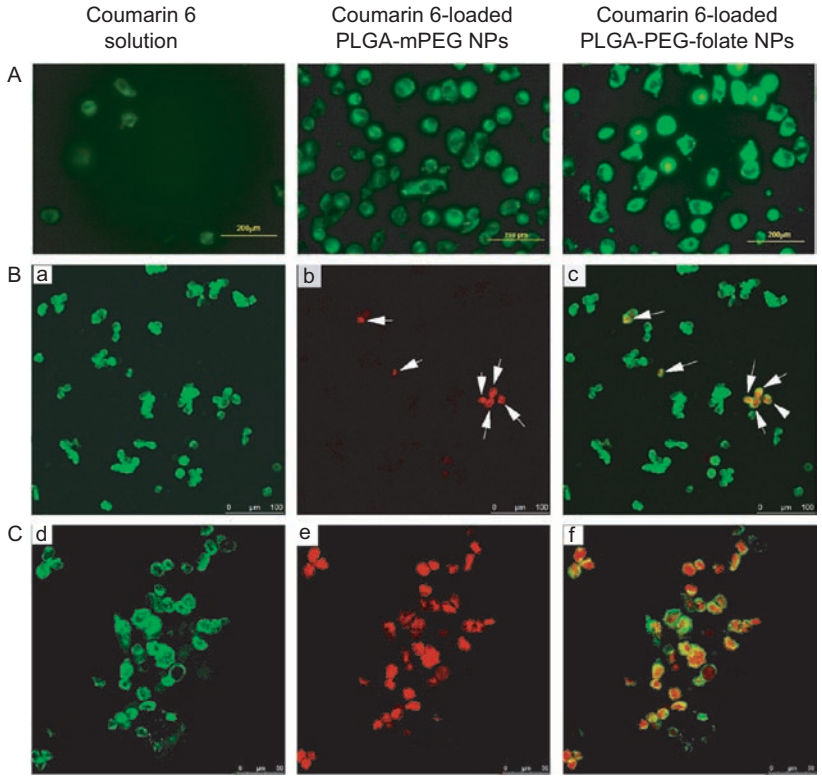

Figure 5. (A) The fluorescence images of MCF-7 cells treated with coumarin 6 solution or coumarin 6–loaded nanoparticles (green) in MCF-7 cells. The confocal laser scanning microscopy images of MCF-7 cells treated with VCR-loaded PLGA–PEG–folate NPs for 1 h (B) and 4 h (C). The cells were stained by propidium iodide (red) and coumarin 6 (green) was visualized by overlaying images obtained by FITC filter and PI filter. (c, f—image from combined PI channel and FITC channel; b, e—image from PI channel; a, d—image from FITC channel). The images show that the red fluorescence intensity increases with the increase of the incubation time within the first 4 h. NP, nanoparticle; PEG, polyethylene glycol; PLGA, poly(lactic-co-glycolic acid); VCR, vincristine sulfate.

for PLGA–PEG–folate NPs. That is, the *in vitro* cytotoxicity of PLGA–PEG–folate NPs was 1.52 and 3.91 times than that of PLGA–mPEG NPs and F-VCR, respectively. The percent viabilities of MCF-7 cells after treatment with F-VCR, PLGA–mPEG NPs, and PLGA–PEG–folate NPs at a concentration of 5 nM were 58.05 ± 4.33%, 42.86 ± 4.01%, and 35.36 ± 2.28%, respectively. Compared with PLGA–PEG–folate NPs, PLGA–mPEG NPs were taken up *via* a nonspecific internalization manner. However, as the above described, the specific conjugation of folic acid with folic acid receptor enabled PLGA–PEG–folate NPs to more easily accumulate within MCF-7 cells, increased cytotoxicity of folate-modified NPs was observed.

To investigate the cytotoxicity of the polymeric carriers, the blank NPs (without VCR encapsulated) with or without the folic acid modification were incubated with MCF-7 cells and the results are shown in Figure 6B. The NPs concentrations were adjusted to 25, 50, 75, and 100 μg/mL, respectively. It can be seen that the cell viability for the blank PLGA–mPEG NPs is 98.35 ± 1.38%, 94.02 ± 0.69%, 90.69 ± 1.44%, and 88.33 ± 1.22% for 24 h, respectively (the 1st column of each group), which means that the cytotoxicity of the blank PLGA–mPEG NPs against MCF-7 cancer cells is almost negligible. The viability for the blank PLGA–PEG–folate NPs can be found to be 98.66 ± 1.68%, 95.31 ± 1.21%, 91.02 ± 0.91 %, and 89.65 ± 0.84%, respectively (the 2nd column of each group), which proves that the folic acid modification on the surface of the blank PLGA–PEG NPs have less/no cytotoxic effects. The above results indicate that the enhanced cellular uptake is responsible for the increased cytotoxic effects of PLGA–PEG–folate NPs whose surface is modified with folic acid. We can conclude that PLGA–PEG–folate NPs loaded with VCR can achieve higher *in vitro* therapeutic effect than F-VCR and PLGA–mPEG NPs do.

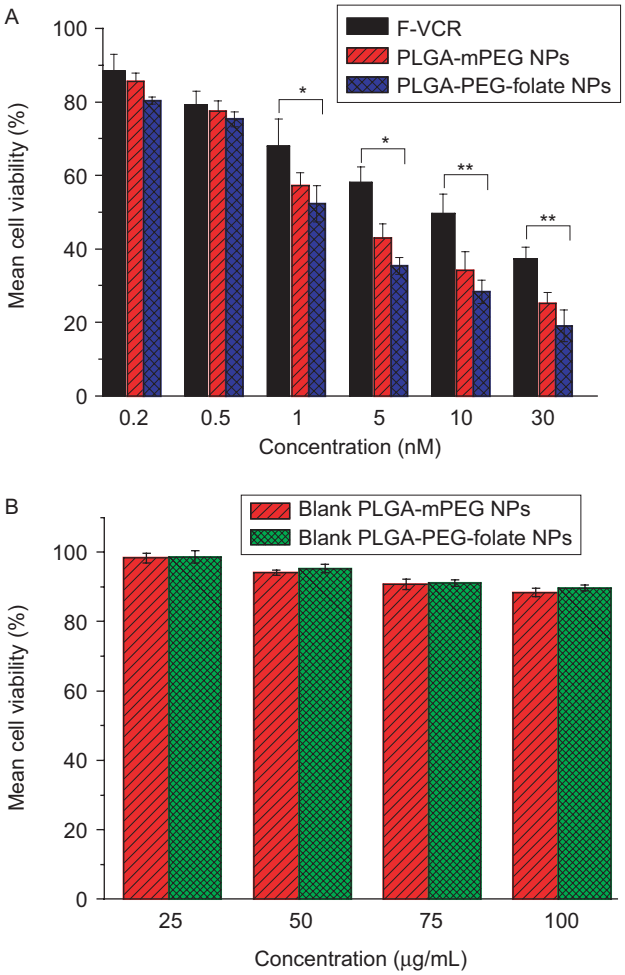

Figure 6. (A) *In vitro* cytotoxicity of F-VCR and VCR-loaded NPs on MCF-7 human breast cancer cells. (B) The cytotoxicity of blank NPs on MCF-7 cells. The cytotoxicity was determined using MTT assay at 37°C for 24 h. In figure (B), the concentrations refer to the total concentrations of the polymeric carriers. Data present as mean ± S.D. ($n=4$). *$p<0.05$; **$p<0.01$. NP, nanoparticle; PEG, polyethylene glycol; PLGA, poly(lactic-co-glycolic acid); VCR, vincristine sulfate.

Conclusion

A VCR-loaded PLGA–PEG drug delivery system, PLGA–PEG–folate NPs, was successfully prepared. The particle size, ζ potential, and morphology obtained were all favorable. The encapsulation of VCR led to a steady release from the NPs for up to 60 h. The folate-modified PLGA–PEG NPs showed significant *in vitro* targeting effects for MCF-7 breast cancer cells, which resulted in enhanced cellular uptake and higher cytotoxicity in comparison with the free drug and PLGA–mPEG NPs. Our results imply that the VCR-loaded PLGA–PEG–folate NPs could have high potentials to be used for targeted chemotherapy. However, the *in vivo* pharmacokinetics, pharmacodynamics, and final biodistribution of NPs also need to be confirmed in future studies.

Acknowledgments

We would like to thank Drs. Tian Lan and Wen Zhou (School of Pharmacy, Shanghai Jiao Tong University) for their advice on synthesis.

Declaration of interest

This work was supported by the National Natural Science Foundation of China (grant no. 30973644), the National Basic Research Program of China (973 Program), No. 2007CB936004, and the National comprehensive technology platforms for innovative drug (R&D, 2009ZX09301-007). The authors report no conflicts of interest. The authors alone are responsible for the content and writing of this paper.

References

1. van Vlerken LE, Vyas TK, Amiji MM. (2007). Poly(ethylene glycol)-modified nanocarriers for tumor-targeted and intracellular delivery. Pharm Res, 24:1405–1414.
2. Wang Z, Chui WK, Ho PC. (2009). Design of a multifunctional PLGA nanoparticulate drug delivery system: Evaluation of its physicochemical properties and anticancer activity to malignant cancer cells. Pharm Res, 26:1162–1171.

3. Wang M, Thanou M. (2010). Targeting nanoparticles to cancer. Pharmacol Res, 62:90–99.
4. Hilgenbrink AR, Low PS. (2005). Folate receptor-mediated drug targeting: From therapeutics to diagnostics. J Pharm Sci, 94:2135–2146.
5. Kim S, Lee J. (2011). Folate-targeted drug-delivery systems prepared by nano-comminution. Drug Dev Ind Pharm, 37:131–138.
6. Saul JM, Annapragada AV, Bellamkonda RV. (2006). A dual-ligand approach for enhancing targeting selectivity of therapeutic nanocarriers. J Control Release, 114:277–287.
7. Zhao D, Zhao X, Zu Y, Li J, Zhang Y, Jiang R, Zhang Z. (2010). Preparation, characterization, and *in vitro* targeted delivery of folate-decorated paclitaxel-loaded bovine serum albumin nanoparticles. Int J Nanomed, 5:669–677.
8. Stella B, Arpicco S, Peracchia MT, Desmaële D, Hoebeke J, Renoir M, D'Angelo J, Cattel L, Couvreur P. (2000). Design of folic acid-conjugated nanoparticles for drug targeting. J Pharm Sci, 89:1452–1464.
9. Cil T, Altintas A, Tamam Y, Battaloglu E, Isikdogan A. (2009). Low dose vincristine-induced severe polyneuropathy in a Hodgkin lymphoma patient: A case report (vincristine-induced severe polyneuropathy). J Pediatr Hematol Oncol, 31:787–789.
10. Moore A, Pinkerton R. (2009). Vincristine: Can its therapeutic index be enhanced? Pediatr Blood Cancer, 53:1180–1187.
11. Rodriguez MA, Pytlik R, Kozak T, Chhanabhai M, Gascoyne R, Lu B, Deitcher SR, Winter JN; Marqibo Investigators. (2009). Vincristine sulfate liposomes injection (Marqibo) in heavily pretreated patients with refractory aggressive non-Hodgkin lymphoma: Report of the pivotal phase 2 study. Cancer, 115:3475–3482.
12. Ravi Kumar MN, Bakowsky U, Lehr CM. (2004). Preparation and characterization of cationic PLGA nanospheres as DNA carriers. Biomaterials, 25:1771–1777.
13. Lü JM, Wang X, Marin-Muller C, Wang H, Lin PH, Yao Q, Chen C. (2009). Current advances in research and clinical applications of PLGA-based nanotechnology. Expert Rev Mol Diagn, 9:325–341.
14. Diao YY, Han M, Ding PT, Chen DW, Gao JQ. (2010). DOX-loaded PEG-PLGA and Pluronic copolymer composite micelles enhances cytotoxicity and the intracellular accumulation of drug in DOX-resistant tumor cells. Pharmazie, 65:356–358.
15. Kamaly N, Kalber T, Thanou M, Bell JD, Miller AD. (2009). Folate receptor targeted bimodal liposomes for tumor magnetic resonance imaging. Bioconjugate Chem, 20:648–655.
16. Shi G, Guo W, Stephenson SM, Lee RJ. (2002). Efficient intracellular drug and gene delivery using folate receptor-targeted pH-sensitive liposomes composed of cationic/anionic lipid combinations. J Control Release, 80:309–319.
17. Wang H, Zhao P, Liang X, Gong X, Song T, Niu R, Chang J. (2010). Folate-PEG coated cationic modified chitosan–cholesterol liposomes for tumor-targeted drug delivery. Biomaterials, 31:4129–4138.
18. Hattori Y, Maitani Y. (2004). Enhanced *in vitro* DNA transfection efficiency by novel folate-linked nanoparticles in human prostate cancer and oral cancer. J Control Release, 97:173–183.
19. Pan J, Feng SS. (2008). Targeted delivery of paclitaxel using folate-decorated poly(lactide)-vitamin E TPGS nanoparticles. Biomaterials, 29:2663–2672.
20. Lee ES, Na K, Bae YH. (2005). Doxorubicin loaded pH-sensitive polymeric micelles for reversal of resistant MCF-7 tumor. J Control Release, 103:405–418.
21. Zhao H, Yung LY. (2008). Selectivity of folate conjugated polymer micelles against different tumor cells. Int J Pharm, 349:256–268.
22. Song XR, Cai Z, Zheng Y, He G, Cui FY, Gong DQ, Hou SX, Xiong SJ, Lei XJ, Wei YQ. (2009). Reversion of multidrug resistance by co-encapsulation of vincristine and verapamil in PLGA nanoparticles. Eur J Pharm Sci, 37:300–305.
23. Avgoustakis K, Beletsi A, Panagi Z, Klepetsanis P, Livaniou E, Evangelatos G, Ithakissios DS. (2003). Effect of copolymer composition on the physicochemical characteristics, *in vitro* stability, and biodistribution of PLGA-mPEG nanoparticles. Int J Pharm, 259:115–127.
24. Beletsi A, Leontiadis L, Klepetsanis P, Ithakissios DS, Avgoustakis K. (1999). Effect of preparative variables on the properties of poly(DL-lactide-co-glycolide)-methoxypoly(ethyleneglycol) copolymers related to their application in controlled drug delivery. Int J Pharm, 182:187–197.
25. Esmaeili F, Ghahremani MH, Ostad SN, Atyabi F, Seyedabadi M, Malekshahi MR, Amini M, Dinarvand R. (2008). Folate-receptor-targeted delivery of docetaxel nanoparticles prepared by PLGA-PEG-folate conjugate. J Drug Target, 16:415–423.
26. Wang L, Wang S, Bei Jz. (2004). Synthesis and characterization of macroinitiator-amino terminated PEG and poly(γ-benzyl-L-glutamate)-PEO-poly(γ-benzyl-L-glutamate) triblock copolymer. Polym Advan Technol, 15: 617–621.
27. Yoo HS, Park TG. (2004). Folate receptor targeted biodegradable polymeric doxorubicin micelles. J Control Release, 96:273–283.
28. Cohen-Sela E, Teitlboim S, Chorny M, Koroukhov N, Danenberg HD, Gao J, Golomb G. (2009). Single and double emulsion manufacturing techniques of an amphiphilic drug in PLGA nanoparticles: Formulations of mithramycin and bioactivity. J Pharm Sci, 98:1452–1462.
29. Meng FT, Ma GH, Qiu W, Su ZG. (2003). W/O/W double emulsion technique using ethyl acetate as organic solvent: Effects of its diffusion rate on the characteristics of microparticles. J Control Release, 91:407–416.
30. Sheshala R, Peh KK, Darwis Y. (2009). Preparation, characterization, and *in vivo* evaluation of insulin-loaded PLA-PEG microspheres for controlled parenteral drug delivery. Drug Dev Ind Pharm, 35:1364–1374.
31. Cavalli R, Donalisio M, Civra A, Ferruti P, Ranucci E, Trotta F, Lembo D. (2009). Enhanced antiviral activity of Acyclovir loaded into β-cyclodextrin-poly(4-acryloylmorpholine) conjugate nanoparticles. J Control Release, 137:116–122.
32. Hu K, Li J, Shen Y, Lu W, Gao X, Zhang Q, Jiang X. (2009). Lactoferrin-conjugated PEG-PLA nanoparticles with improved brain delivery: *In vitro* and *in vivo* evaluations. J Control Release, 134:55–61.
33. Davda J, Labhasetwar V. (2002). Characterization of nanoparticle uptake by endothelial cells. Int J Pharm, 233:51–59.
34. Win KY, Feng SS. (2005). Effects of particle size and surface coating on cellular uptake of polymeric nanoparticles for oral delivery of anticancer drugs. Biomaterials, 26:2713–2722.
35. Stella B, Marsaud V, Arpicco S, Géraud G, Cattel L, Couvreur P, Renoir JM. (2007). Biological characterization of folic acid-conjugated poly(H2NPEGCA-co-HDCA) nanoparticles in cellular models. J Drug Target, 15:146–153.
36. Wu L, Tang C, Yin C. (2010). Folate-mediated solid-liquid lipid nanoparticles for paclitaxel-coated poly(ethylene glycol). Drug Dev Ind Pharm, 36:439–448.
37. Pinhassi RI, Assaraf YG, Farber S, Stark M, Ickowicz D, Drori S, Domb AJ, Livney YD. (2010). Arabinogalactan-folic acid-drug conjugate for targeted delivery and target-activated release of anticancer drugs to folate receptor-overexpressing cells. Biomacromolecules, 11:294–303.
38. Yang SJ, Lin FH, Tsai KC, Wei MF, Tsai HM, Wong JM, Shieh MJ. (2010). Folic acid-conjugated chitosan nanoparticles enhanced protoporphyrin IX accumulation in colorectal cancer cells.. Bioconjugate Chem, 21:679–689.